Mononuclear $[(BP)_2MX]^{n+}$ ($M = Cu^{2+}, Co^{2+}, Zn^{2+}; X = OH_2, Cl^-$) complexes with a new biphenyl appended N-bidentate ligand: structural, spectroscopic, solution equilibrium and ligand dynamic studies†

Shahulhameed Sabiah,*‡[a] Babu Varghese[b] and Narasimha N. Murthy[a]

Received 28th May 2009, Accepted 1st September 2009
First published as an Advance Article on the web 28th September 2009
DOI: 10.1039/b910519k

A new series of five-coordinate $[(BP)_2MX]^{n+}$ complexes, (where $X = OH_2$, $M = Zn(II)$ (**1**), Cu(II) (**2**); $X = Cl^-$, $M = Cu(II)$ (**3**), Co(II) (**4**)) with a new bidentate chelating ligand [{N,N(1,1′-biphenyl-2,2′-dimethylene)-N(2-pyridyl methyl)} amine] with a biphenyl group (BP), have been synthesized and characterized by X-ray crystal structure and combined spectroscopic methods. They display unique trigonal bipyramidal (TBP) geometry, influenced by the bidentate ligand. The Zn(II) complex **1** reveals ligand dynamics due to an atropisomeric biphenyl moiety as indicated by variable temperature (VT) proton NMR spectroscopy. The calculated free energy for the inversion of the bridged biphenyl is ~13.08 kcal mol^{-1} ($T_c = 273$ K, $\Delta\nu = 82.8$ Hz, $J = 8.7$ Hz). The absorption spectra of Cu(II) complexes **2** and **3**, in CH_2Cl_2 display greatly enhanced d–d bands (800–950 nm, $\varepsilon > 500$ M^{-1} cm^{-1}). On the other hand, complex **2** in N,N-dimethylformamide (DMF) showed almost 50% reduction in absorption intensity as DMF, a coordinating solvent, displaces the weakly-coordinated tertiary amine-nitrogens of the ligand and this competitive binding was studied by electronic absorption spectroscopy. When the mononuclear copper aqua complex **2** was treated with a base, a dicopper dihydroxide complex, $[\{(BP)Cu\}_2(\mu\text{-}OH)_2]^{2+}$, (**2a**) was obtained. The same phenomenon was also observed with chloro complex **3** when treated with a base. This mono-dicopper equilibrium and conversion of **2** → **2a** was monitored by UV-vis spectroscopy. Copper(II) complexes **2** and **3** displayed "reverse" EPR spectra consistent with the TBP geometry. Cyclic voltammetry of **2** and **3** in DMF showed an irreversible redox wave owing to Cu(II)/Cu(I) of five and four-coordinate species. The solution magnetic moment values of 1.76, 1.81 and 4.47 μB for **2**, **3** and **4**, respectively, are in agreement with Cu(II) ($S = 1/2$) and Co(II) ($S = 3/2$) high-spin configurations. The ^1H NMR of **4** displays sharp but hyperfine shifted signals for the ligand protons between −30 to +220 ppm. The ESI-mass data complement the data obtained from X-ray structure.

Introduction

Mononuclear metal centers play important roles in natural and synthetic catalytic systems. They are essential active site components in a number of metalloenzymes such as dopamine β-monooxygenase (DBM), peptidylglycine α-hydroxylating monooxygenase (PHM), carbonic anhydrase (CA) and carboxypeptidase (CP) and so on.[1–3] The minute differences in the active sites of these enzymes bring diverse activities. Largely, the ligand environments around the metal centers dictate the active site geometric perturbations to bring unusual spectral properties and in many cases enhanced catalytic activities.[4,5] Hence, as a first step, intensive investigations have been carried out on simple model complexes to tune the desired geometries as modulated by the ligands.[6] It has been demonstrated that sterically and electronically demanding pyridyl ligands such as tmpa (tmpa = tris(2-pyridylmethyl)amine) and their derivatives can dictate the coordination geometry, and redox potential which are extensively employed in activation of small molecules.[5] Similarly, other conventional ligands such as tren (tren = tris(2-aminoethyl)amine), the tridentate ligands, tris-pyrazolyl borates, tacn (tri-aza-cyclononane) and the bidentate ligands, cyclohexyl diamine, peralkylated diamine, β–diketiminate,[5,7] and polyamine[8] bidentate ligands are widely studied. However, the biaryl armed nitrogenous ligands are scarce in coordination chemistry.[9] Nevertheless, these ligands are often employed as chiral auxiliaries in asymmetric synthesis.[10] Hence there is ample interest in the design and synthesis of new transition metal-ion complexes with the flexible biaryl ligands with multidentate nitrogen donors.

Here, we report the crystal structures and comparative spectroscopic (NMR, UV-vis, EPR and ESI-MS) properties of $[(BP)_2Zn(OH_2)](ClO_4)_2$ (**1**), $[(BP)_2Cu(OH_2)](ClO_4)_2$ (**2**), $[(BP)_2CuCl](ClO_4)$ (**3**), $[(BP)_2CoCl](ClO_4)$ (**4**) and $[(BP)_2CoCl]Br$ (**5**), including their solution magnetic data. We have utilized a new N,N bidentate ligand with biphenyl backbone, BP (Fig. 1),

---

[a] *Department of Chemistry, Indian Institute of Technology, Madras, India. E-mail: sabiahs@gmail.com; Fax: +886 3 8632000*
[b] *Sophisticated Analytical Instrumentation Facility, Indian Institute of Technology, Madras, India*

† Electronic supplementary information (ESI) available: CCDC reference numbers 645339–645341. For ESI and crystallographic data in CIF or other electronic format see DOI: 10.1039/b910519k

‡ Current address: Department of Chemistry, National Dong Hwa University 1, Section 2, Da-Hsueh Road, Hualien 974, Taiwan, ROC.

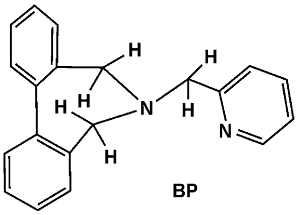

Fig. 1 Chemical structure of BP.

to study the coordination properties of these transition metal-ion complexes.

Originally, we focused our studies on biomimetic model complexes of BP and during the course of our efforts, we have found that these series of metal complexes have a unique geometry with ligand enforced C_2 symmetry (Fig. 2). Interestingly, by designing the new bidentate ligand, we have introduced (i) steric crowding near the tertiary amine-nitrogen donor sites, (ii) unique geometry around the metal centers and (iii) flexibility in the MN_4 coordinated unit.

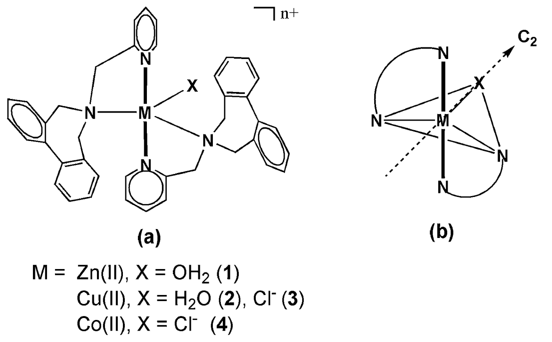

Fig. 2 (a) Trigonal bipyramidal geometry and (b) crystallographic C_2-symmetry enforced by ligand, BP.

The structures of these complexes with TBP geometry represent the first structural proof of Cu(II), Zn(II) and Co(II) with an aminopyridyl ligand containing biphenyl appendage. Also the VT-^{1}H NMR spectroscopy of the zinc complex **1**, shows biaryl atropisomeric ligand dynamics in solution. The competitive binding studies of the Cu(II)-aqua complex, **2** with N,N-dimethylformamide (DMF) proposes the possible ligand hemilability. In addition, an attempted synthesis of the mononuclear hyrdoxide-analogue of **2**, *i.e.* $[(BP)_2Cu(OH)]^+$ gave instead the dihydroxide-bridged dinuclear complex, $[\{(BP)Cu\}_2(\mu\text{-}OH)_2]^{2+}$ **2a**, and this rare conversion of **2** → **2a** monitored by UV-vis spectroscopy is also discussed.

Experimental

Physical measurements

All chemicals and solvents were of commercially available reagent grade quality. Solvents were dried and distilled by standard procedures prior to use.[11] C, H, N analyses was performed on a Perkin-Elmer 2400 Series CHNS/O Analyzer. Electronic absorption spectra were recorded on a CARY 5E model and FTIR spectra as KBr disks on a Shimadzu IR-470 spectrophotometer. Proton NMR spectra were recorded either on a BRUKER AVANCE-400 or a JEOL GMX-400 spectrometer. Room temperature magnetic moments of metal complexes were calculated by Evans method[12] in an appropriate deuteriated solvent. EPR spectra were obtained from a Varian E-112 X-band spectrometer as frozen-glass at 77 K. Mass spectra were obtained in acetonitrile or water mixture on a Q-Tof-Mass Spectrometer equipped with a standard electrospray source. Electrochemical measurements were performed on Bio-Analytical Systems (BAS 100A) electrochemical analyzer. A cell equipped with a glassy carbon working electrode, a Pt-wire auxiliary electrode and Ag/AgCl reference electrode, fitted with a Vycor plug at the solution junction, and a nozzle for bubbling of N_2, was used.

Syntheses of metal complexes.

Safety Note: *Caution! Although we have experienced no problems with the metal complexes of perchlorate salt, they are potentially explosive and should be handled with care.*

The ligand BP was prepared by our group.[13]

$[(BP)_2Zn(H_2O)](ClO_4)_2$, 1. To a solution of zinc perchlorate hexahydrate (0.25 g, 0.65 mmol) in ethanol (5 mL), was added a solution of ligand BP (0.38 g, 1.33 mmol) in the same solvent (6 mL). A pale yellowish-white precipitate that formed was stirred for 2 h, filtered and dried *in vacuo* to yield **1** (0.42 g, 76%). X-Ray quality crystals were obtained by slow evaporation of the solution of complex **1**, in acetonitrile and ethanol (1 : 1, v/v). Anal. Calcd for $C_{40}H_{38}Cl_2Zn_2N_4O_9$: C, 56.18; H, 4.48; N, 6.55. Found: C, 56.06; H, 4.43; N, 6.56%. ^{1}H NMR (δ, CD_3CN, 400 MHz, 293 K): 2.72 (bs, H_2O), 3.65 (s, 4H, CH_2biphenyl), 4.41 (s, 2H, CH_2Py), 7.30–7.74 (m, 10H, aromatic), 8.06 (s, 1H, py-H4); ^{13}C NMR (δ, CD_3CN, 100.61 MHz): 57.3, 60.9, 126.4, 126.6, 129.8, 130.0, 131.4, 132.3, 142.5, 149.9, 154.2 ppm. UV-vis (CH_3CN; λ_{max}, nm (ε, M^{-1} cm^{-1}) 248 (37 375). FT-IR (KBr, cm^{-1}): 3420 (bs), ν(coordinated OH_2); 1094 (bs), $\nu(ClO_4)$. ESI-MS (CH_3CN/H_2O): *m/z* 635, Zn + 2L; *m/2z* 349 (7%), $[(BP)_2Zn(OH_2)(CH_3CN)]_2^{2+}$; *m/2z* 390 (9%), $\{[(BP)_2Zn\ (OH_2)(CH_3CN)]_2^{2+} + CH_3CN\}$; *m/z* 448 (12%), $[BPZn(ClO_4)]^+$; *m/z* 287 (100%), $[BP + H]^+$.

$[(BP)_2Cu(H_2O)](ClO_4)_2$, 2. To a stirred solution of copper perchlorate hexahydrate (0.14 g, 0.37 mmol) in ethanol (7 mL), was added, drop wise, a solution of ligand BP (0.22 g, 0.75 mmol) in ethanol (4 mL). The resulting green precipitate was allowed to stir for 1 h, filtered and dried *in vacuo* to obtain **2** (0.29 g, 89%). X-Ray quality crystals were obtained by slow evaporation of the solution of complex **2**, in dichloromethane and ethanol (1 : 1, v/v). Anal. Calcd for $C_{40}H_{38}Cl_2CuN_4O_9$: C, 56.77; H, 4.37; N, 6.64. Found: C, 56.31; H, 4.48; N, 6.56%. UV-vis [CH_2Cl_2, λ_{max}, nm (ε, M^{-1} cm^{-1})]: 398 (1250), 827 (586), 950 (530); FT-IR (KBr, cm^{-1}): 3420 (bs), ν(coordinated OH_2); 1094 (bs), $\nu(ClO_4)$. μ_B (Evans, CD_3CN, 298 K): 1.76 BM/Cu(II). EPR (CH_2Cl_2 : toluene, 1 : 1, v/v, 77 K): $g_1 = 2.233$, $g_2 = 2.064$, $g_3 = 2.020$. ESI-MS (CH_3CN/H_2O): *m/z*, 734 (8%), $[M - ClO_4]^+$; *m/z* 287 (100%), $[BP + H]^+$.

$[(BP)_2Cu(Cl)](ClO_4)\cdot H_2O$, 3·$H_2O$. To a solution of cupric chloride dihydrate (0.05 g, 0.29 mmol) and BP (0.16 g, 0.58 mmol) in ethanol (10 mL), was introduced sodium perchlorate (0.03 g, 0.29 mmol) in the same solvent (5 mL). A green precipitate, which formed was allowed to stir for 1 h, filtered and dried *in vacuo* to give **3** (0.19 g, 85%). X-Ray quality crystals were obtained by slow evaporation of the solution of **3**, in dichloromethane and ethanol (1 : 1, v/v). Anal. Calcd for $C_{40}H_{36}Cl_2CuN_4O_4$: C, 62.29; H, 4.70;

N, 7.26. Found: C, 61.44; H, 4.76; N, 7.15%. UV-vis [CH_2Cl_2, λ_{max}, nm (ε, M^{-1} cm^{-1})]: 369 (1948), 824 (587), 964 (650). FT-IR (KBr, cm^{-1}): 3487 (b), ν(lattice OH_2); 1097 (bs), ν(ClO_4). μ_B (Evans, CD_3NO_2, 298 K): 1.81 BM/Cu(II). EPR (CH_2Cl_2 : toluene, 1 : 1, v/v, 77 K): $g_{\parallel}$ = 1.987, $A_{\parallel}$ = 85(G); $g_{\perp}$ = 2.200, $A_{\perp}$ = 90(G). ESI-MS (CH_3CN/H_2O): *m/z* 670 (62%), M^+; *m*/2*z* 384 (85%), $[BPCu(Cl)]_2^{2+}$; *m/z* 287 (100%), $[(BP + H)]^+$.

$[(BP)_2Co(Cl)](ClO_4)$, 4. To an ethanol (4 mL) solution of $CoCl_2 \cdot 6H_2O$ (0.07 g, 0.29 mmol) was added the solution of BP (0.16 g, 0.56 mmol) in the same solvent (6 mL), followed by an ethanolic solution of $NaClO_4$ (0.07 g, 0.45 mmol). The resulting blueish purple precipitate was allowed to stir for 1 h, filtered and dried *in vacuo* to obtain **4** (0.22 g, 82%). Anal. Calcd for $C_{40}H_{36}Cl_2CoN_4O_4$: C, 62.75; H, 4.74; N, 7.61. Found: C, 62.85; H, 4.94; N, 7.80%. UV-vis [CH_2Cl_2, λ_{max}, nm (ε, M^{-1} cm^{-1})]: 481 (74), 520 (90), 640 (79), 848 (51). FT-IR (KBr, cm^{-1}): 1101 (bs), ν(ClO_4). μ_B (Evans, $CDCl_3$, 298 K): 4.47 BM/Co(II). ^1H NMR (δ, $CDCl_3$, 400 MHz): −28.3, −6.2, 5.4, 8.1, 8.9, 9.5, 14.2, 14.8, 20.9, 22.4, 32.4, 35.1, 46.0, 48.6, 74.5, 82.3, 202.9, 220.6 ppm. ESI-MS (CH_3CN/H_2O): *m/z* 666 (37%), M^+; *m*/2*z* 380 (9%), $[BPCo(Cl)]_2^{2+}$; *m/z* 287 (100%), $[(BP + H)]^+$.

X-Ray crystallography. X-Ray crystallographic studies were carried out on a Enraf-Nonius CAD-4 diffractometer[14] equipped with Mo Kα (λ = 0.7107 Å) or Cu Kα (λ = 1.541 Å) radiation. The intensity data were corrected for Lorentzian polarization and absorption effects. The structures were solved by direct method (SHELXL-97)[15] and refined by full-matrix least squares techniques using SIR92 program.[16] All hydrogen atoms except for coordinated H_2O were fixed at chemically meaningful positions and riding model refinement was applied. The coordinated water hydrogens were located through difference Fourier map and refined with isotropic thermal parameter. The Zn, Cu and O1 atoms of **1** and **3** sit on a special position, C_2 symmetry. The ClO_4 oxygens of **1**, **2** and **3** have positional disorder. In **1**, all the four oxygens are statistically disordered about six positions. On the other hand, in **2** the disorder is about nine positions; while, in complex **3**, both chlorine and oxygen atoms are disordered. The multiplicity factors for each of the oxygen atoms were chosen such that the total multiplicities for each site were unity. Molecular graphics were generated using either DIAMOND or WINGX programs.[17]

Results and discussion

1. The ligand (BP) and its complexes

The ligand (BP) is a chelating bidentate. It is a derivative of (2-pyridylmethyl)amine, in which the amine-end is appended to sterically demanding 2,2′-dimethylene-1,1′-biphenyl group (Fig. 1). It has three methylene bridges linking the pyridyl and biphenyl rings *via* tertiary amine-N. The pair of hydrogens on each methylene are diastereotopic. The three-atom (C–N–C) bridged biphenyl forms a seven-membered ring and exhibits conformational flexibility in solution. However, when bonded to a metal center, it may be rigid and such rigid molecules with a biphenyl group serve as chiral auxiliaries in the asymmetric synthesis.[10] The ligand provides pyridyl and tertiary-amino nitrogen donor atoms for ligation, with restricted accessibility of the amino-N because of the steric obstruction from the biphenyl group. The ligand offers combined electronic and steric effects through a strong σ-donor pyridyl group, and a weak donor tertiary amine-nitrogen due to the bulky biphenyl group. It renders flexible non-planar chelation around the metal centers leading to unique control over coordination geometry. The reaction of the 1 : 2 ratio of M(II) salts, (M = Cu, Co, Zn,) and BP in ethanol yielded the mononuclear complexes, **1–5** in moderate to good yields, as shown for the case of Cu(II) complex **2** (eqn (1)):

$$2BP + Cu(ClO_4)_2 \cdot 6H_2O \xrightarrow{EtOH} [(BP)_2Cu(H_2O)](ClO_4)_2, \mathbf{2} \quad (1)$$

2. Crystal structures

Single crystals of the zinc and cobalt complexes **1** and **5** were obtained from acetonitrile and ethanol by slow evaporation of solvents. Pale green needles of the cupric complexes **2** and **3·H_2O** were obtained from CH_2Cl_2/EtOH. The structure of cobalt(II) complex $[(BP)_2Co(Cl)]Br$, **5** has been reported.[18] A perspective view of the coordination environment of metal-ions in **1**, **2** and **3** is shown in Fig. 3(a)–(c). Crystal data, selected bond distances and angles and important geometric parameters around each metal are provided in Tables 1–3.

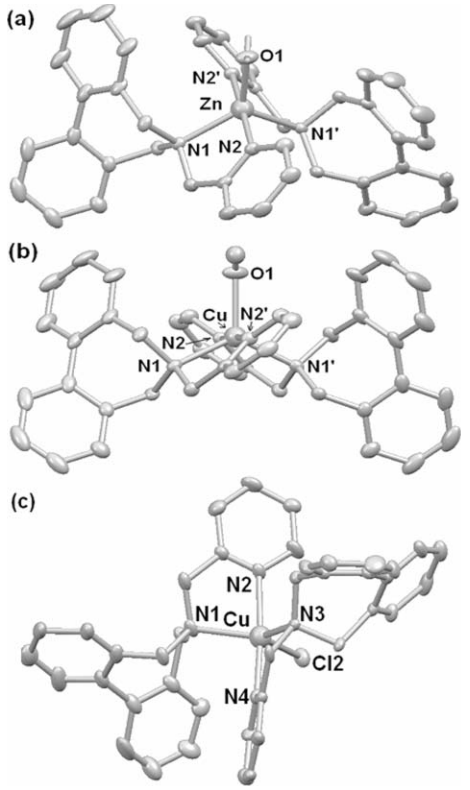

Fig. 3 (a)–(c) Diamond view of the crystal structures of complexes **1**, **2** and **3** at 40% ellipsoid probability.

Molecules **1**, **2** and **5** lie down on a crystallographic C_2-symmetry, along the M–X vector, bisecting each molecule into two equal-halves (Fig. 2); while **3** contains a pseudo-C_2 axis. The metal ions are five-coordinated with trigonal bipyramidal geometry, with ligation from pyridyl, tertiary amino-nitrogens, and an aqua (H_2O) or chloride (Cl^-) anion. In each case, the tertiary amine-nitrogen binds the metal along the equatorial plane

Table 1 Crystallographic data for **1**, **2** and **3**·H_2O

Compound	**1**	**2**	**3**·H_2O
Molecular formula	$C_{40}H_{38}Cl_2ZnN_4O_9$	$C_{40}H_{38}Cl_2CuN_4O_9$	$C_{40}H_{37}Cl_2CuN_4O_{4.5}$
Formula weight	855.01	853.18	780.18
Temp/K	293	293	293
Crystal system	Monoclinic	Monoclinic	Orthorhombic
Space group	*C*2/*c*	*C*2/*c*	*Pbca*
Z	4	4	8
a/Å	22.156(5)	22.153(12)	9.342(2)
b/Å	9.8328(17)	9.755(2)	21.1380(19)
c/Å	20.202(2)	22.365(6)	37.486(6)
α/°	90	90	90
β/°	115.408(13)	124.36(3)	90
γ/°	90	90	90
V/Å^3	3975.4(11)	3990(3)	7402(2)
λ/Å	0.7107	0.7107	1.5418
D_c/mg m^{-3}	1.429	1.420	1.400
Reflections collected	6164	3485	6723
Reflections used	2409 [$I > 2\sigma(I)$]	2214 [$I > 2\sigma(I)$]	4847 [$I > 2\sigma(I)$]
Abs coeff/mm^{-1}	0.812	0.741	2.554
No. of refined parameters	291	291	522
R^a	0.0613	0.0624	0.0539
$R_w{}^b$	0.1737	0.1750	0.1624

[a] $R = \sum||F_o| - |F_c||/\sum|F_o|$. [b] $R_w = [\sum w(|F_o|^2 - |F_c|^2)/\sum w(F_o{}^2)^2]^{\frac{1}{2}}$; w $=1/[(F_o{}^2)^2 + (0.0652P)^2 + 14.5152P]$ (for **1**); $1/[(F_o{}^2)^2 + (0.0791P)^2 + 7.0101P]$ (for **2**); $1/[(F_o{}^2)^2 + (0.0980P)^2 + 2.4841P]$ (for **3**).

Table 2 Selected bond distances (Å) and bond angles (°) of **1–3**, **5**

1		**2**		**3**·H_2O		**5**	
Distances							
Zn–O1	2.012(6)	Cu1–O1	2.096(5)	Cu1–Cl1	2.330(1)	Co1–Cl1	2.334(14)
Zn–N1	2.151(4)	Cu1–N1	2.155(4)	Cu1–N1	2.178(2)	Co1–N1	2.155(3)
Zn–N2	2.121(4)	Cu1–N2	1.975(4)	Cu1–N2	1.972(3)	Co1–N2	2.133(3)
Zn–N1′	2.151(4)	Cu1–N1′	2.155(4)	Cu1–N3	2.197(2)	Co1–N1′	2.155(3)
Zn–N2′	2.121(4)	Cu1–N2′	1.975(4)	Cu1–N4	1.988(3)	Co1–N2′	2.133(3)
Angles							
N2–Zn–N2′	175.1(2)	N2–Cu1–N2′	176.7(2)	N2–Cu1–N4	170.11(12)	N2–Co1–N2′	171.69(14)
N1–Zn–N1′	121.7(2)	N1–Cu1–N1′	128.14(19)	N1–Cu1–N3	123.86(9)	N1–Co1–N1′	122.24(13)
O1–Zn–N1	119.16(10)	O1–Cu1–N1	115.93(9)	Cl1–Cu1–N1	118.55(7)	Cl1–Co1–N1	118.88(7)
O1–Zn–N1′	119.16(10)	O1–Cu1–N1′	115.93(9)	Cl1–Cu1–N3	117.55(6)	Cl1–Co1–N1′	118.88(7)
O1–Zn–N2	92.43(12)	O1–Cu1–N2	91.63(12)	Cl1–Cu1–N2	92.93(9)	Cl1–Co1–N2	94.15(7)
O1–Zn–N2′	92.43(12)	O1–Cu1–N2′	91.63(12)	Cl1–Cu1–N4	96.86(9)	Cl1–Co1–N2′	94.15(7)
N2–Zn–N1	79.45(16)	N2–Cu1–N1	81.18(16)	N2–Cu1–N1	80.63(10)	N2–Co1–N1	78.73(10)
N2′–Zn–N1′	79.45(16)	N2′–Cu1–N1′	81.18(16)	N4–Cu1–N3	79.35(10)	N2′–Co1–N1′	78.73(10)
N2–Zn–N1′	98.16(15)	N2–Cu1–N1′	97.37(16)	N2–Cu1–N3	94.87(10)	N2–Co1–N1′	97.21(10)
N2′–Zn–N1	98.16(15)	N2′–Cu1–N1	97.37(16)	N4–Cu1–N1	95.88(10)	N2′–Co1–N1	97.21(10)

Table 3 Summary of some important geometric parameters around each metal in **1–3**, **5**

						Dihedral angle (φ)/°			
Complex	β/°	α/°	τ	Geometry	N–N bite angle/°	MN_2/MN_2'	Py/Py′	Biphenyl twist	Ionic radii/Å^a
$[Zn(OH_2)(BP)_2]^{2+}$, **1**	175.1	121.7	0.89	TBP	79.5	58.6	87.1	45	0.68
$[Cu(OH_2)(BP)_2]^{2+}$, **2**	176.7	128.1	0.81	TBP	81.2	52.1	89.6	45.6	0.65
$[CuCl(BP)_2]^{+}$, **3**	170.1	123.9	0.77	TBP	80.6, 79.4	56.5	86.6	46, 42	0.65
$[CoCl(BP)_2]^{+}$, **5**	171.7	122.2	0.83	TBP	78.7	57.8	88.5	42	0.67

[a] For five-coordinate geometry.

and the pyridyl nitrogen along the apical position with average metal–N(amine) bond distances differing significantly from the metal–N(py) in the apical position. The geometrical parameters in the present study are comparable with the analogous five-coordinate complexes with N_4-donor set, like trenMe$_3$ or tpa.[19a]

The common feature in these complexes is the ligand bite angles, N–M–N, (79.4–81.2°) which are within a narrow range observed for analogous metal complexes with bipy (bipy = 2,2′-bipyridine) or phen (1,10-phenanthroline) ligand systems.[19b] Interestingly, the two pyridyl rings are disposed perpendicular to each other

(φ = 86.6 to 89.6°), in sharp contrast to their near coplanar (ϕ = 2–10°) arrangement recognized for mononuclear complexes with bipyridyl ligand systems.[20] This arrangement is probably due to the steric congestion exerted by the biphenyl groups, placed on each tertiary amine-N atoms. The intrinsic non-coplanarity of the aryl rings of biphenyl is apparent from the biaryl twist angle of ~42 to 46° which is comparable with analogous bridged biphenyls.[21,22]

Nevertheless, the bond parameters of biaryl match quite close to the reported biphenyl cores.[23] The dihedral angles between the planes defined by two MN_2 units vary from 52.1 to 56.5°. The sum of equatorial bond angles at Zn is 359.99° showing that the metal ion is essentially in the mean plane of the equatorial donors (N1N1′O1). An important comparison of **1** is to the zinc enzyme astacin, where a Zn–OH_2 unit ligated in a trigonal bipyramidal fashion with water ligand in the equatorial position (Zn–O = 2.1 *vs.* 2.0 Å in **1**).[24]

The Cu–O distance in **2** (2.09 Å) is shorter than that observed in the analogous complex with 1,10-phenanthroline (~2.25 Å) and longer than axially coordinated water in $[(\text{tmpa})Cu(H_2O)]^{2+}$ (~1.98 Å) with TBP geometry.[25] The Cu–Cl distance of **3** (2.33 Å) is in the range observed for $[(\text{phen})_2Cu(Cl)]^+$ (av. ~2.32 Å),[26] $[(\text{bipy})_2Cu(Cl)]^+$ (2.263)[27] and $[(\text{tmpa})Cu(Cl)]^+$ (2.23 Å) complexes.[28] For copper complexes **2** and **3**, the axial Cu–N(py) distances are much shorter than those in **1** and **5**, which is in agreement with the position of copper in the Irving–Williams series. The in-plane bond angles, N_{amine}–M–N_{amine} range from 121.7–128.1°, most deviated for **2**.

Structurally, the five-coordinate complexes range from C_{4v} (square pyramidal) to D_{3h} (trigonal bipyramidal) geometries with conformational rearrangement through classical Berry pathway.[29] An analysis of the geometrical shape determining dihedral angles (φ) about each metal, yield values in the range 49.5–54.8°, 48.9–60.6°, 46.4–64.9° and 45.9–59.3° for **1**, **2**, **3** and **5**, respectively, compared to 53° expected for an ideal TBP geometry.[30] This suggests close to TBP geometry for **1** and distorted geometries for the others. Furthermore, a structural parameter $\tau = (\beta - \alpha)/60$ introduced by Reedijk *et al.*[31] where α and β represent two basal angles $\beta \geq \alpha$, was also adopted to systematize the change in the geometries of the complexes. A perfect trigonal-bipyramidal is associated with $\alpha = 120°$ and $\beta = 180°$ ($\tau = 1$). The structural parameters α, β, and τ are summarized in Table 3. The general structural motif in these five-coordinate complexes is represented as N_4MX. Since we started our work with the main focus on copper systems, we have analyzed the Cambridge Structural Database with N_4CuO and N_4CuCl motifs with either TBP or SPy geometries. There are 1530 and 319 structures with N_4CuO and N_4CuCl motifs, respectively, out of an available 325 709 crystal structures. Since we are interested in N-bidentate chelation, we have narrowed down our search to structures with N-bidentate ligands. The geometries are based on τ values and the results are summarized in Fig. 4. It shows that TBP > SPy in N_4CuO motifs and SPy > TBP in N_4CuCl motifs.

All complexes in the present study show that metal ions adopt unique TBP geometry, with M : BP in 1 : 2 ratio presumably due to ligand constraints. The crystal packing in these complexes reveal strong π–π interaction between two phenyl rings of biphenyl related by inversion symmetry and are placed head-on and parallel. The normal centroid$\cdots$centroid distance between the planes of phenyl is ~3.4 Å. Altogether, the structures are stabilized by π–π and van der Waals interactions.

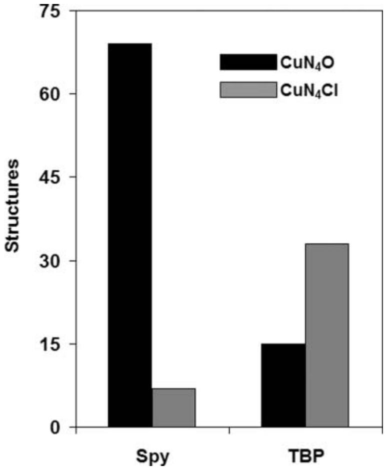

Fig. 4 Square pyramidal and trigonal bipyramidal Cu-geometry distributions with N-bidentate ligands.

3. Solution studies by spectroscopy

(a) Mass spectra. The electrospray ionization (ESI) mass spectra of complexes **1–5** measured in CH_3CN complemented the data obtained from X-ray studies. All of them display two major peaks corresponding to monocationic species. As a representative example, the mass spectrum of $[(BP)_2CuCl](ClO_4)$, **3** is shown in Fig. 5. The peak at *m*/*z* 670 is due to $[(BP)_2Cu(Cl)]^+$ and *m*/*z* 384 is assigned to $[BPCu(Cl)]^+$. The aqua complex, $[(BP)_2Cu(OH_2)](ClO_4)_2$, **2** in acetonitrile–water showed a moderately abundant peak at *m*/*z* 734 due to $[(BP)_2Cu(ClO_4)]^+$. Complex **1** shows a moderately abundant peak at *m*/*z* 448 due to $[BPZn(ClO_4)]^+$ and a peak at *m*/*z* 349 assigned to $[(BP)_2Zn(H_2O)(CH_3CN)]_2^{2+}$ ions. The peak at *m*/*z* 390 may be due to $\{[(BP)_2Zn(H_2O)(CH_3CN)]_2^{2+} + CH_3CN\}$; the peak at *m*/*z* 635 corresponds to $[(BP)_2Zn]^{2+}$ species. For **5**, the fifth site has positional disorder with 2/3 chloride and 1/3 bromide ions. The ESI-MS spectrum of this compound in acetonitrile–MeOH confirms the presence of chloride (666 *m*/*z*) as well as bromide (712 *m*/*z*) in the expected intensity ratio.[18] All complexes show a major peak at *m*/*z* 287, due to $[BP + H]^+$.

(b) UV-vis spectra. Copper(II) complexes with distorted TBP geometry, generally exhibits a broad or twin absorption in the region 700–950 nm, due to $d_{x^2-y^2} \rightarrow d_{z^2}$ and $d_{xy} \approx d_{yz} \rightarrow d_{z^2}$ transitions.[25a] The UV-vis of **2–4** are shown in Fig. 6. The optical absorption spectrum of **2** in CH_2Cl_2, displays a twin peak at 827 (ε = 586 M^{-1} cm^{-1}) and 950 nm (ε = 530 M^{-1} cm^{-1}) with a shoulder at 398 nm. The split band is attested to the TBP geometry as seen in analogous cores.[32] Similarly, **3** exhibits a split band at 824 (ε = 587 M^{-1} cm^{-1}) and 964 nm (ε = 650 M^{-1} cm^{-1}) with a shoulder at 366 nm ($Cl^- \rightarrow$ Cu(II) CT band) comparable to CuN_4Cl motifs.[27] The electronic absorption spectrum of **4** in CH_2Cl_2 shows ligand field transitions at 481, 520, 640 and 848 nm due to ${}^4A_2' \rightarrow {}^4E''(P) + {}^4A_2'(P)$, ${}^4A_2' \rightarrow {}^4E'$, ${}^4A_2' \rightarrow {}^4E''$ and ${}^4A_2' \rightarrow {}^4A_1'' + {}^4A_2''$ (d–d transitions) of TBP high-spin Co(II).[33]

(c) DMF binding and hemilability of BP in $[(BP)_2Cu(OH_2)](ClO_4)_2$. Ligands are said to be hemilabile when one of their

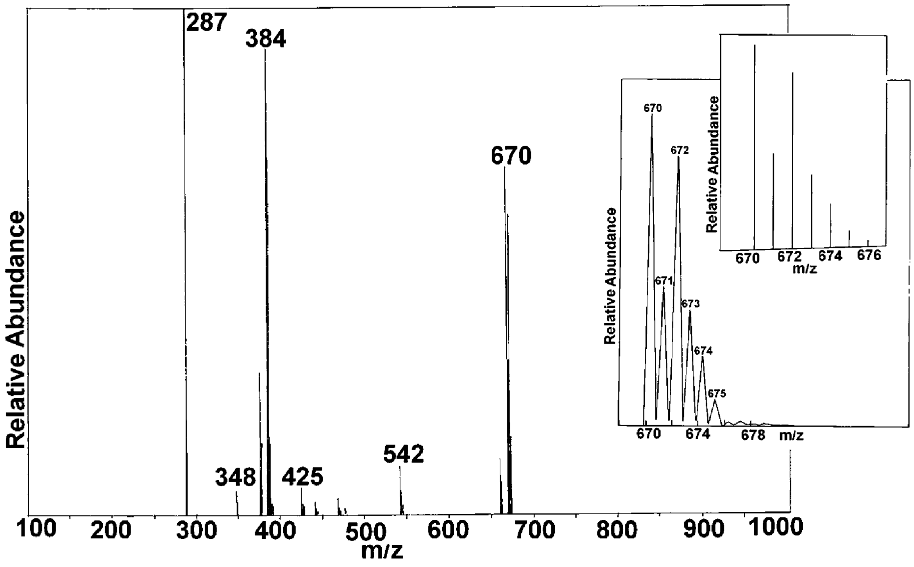

Fig. 5 ESI mass spectrum of $[(BP)_2)CuCl](ClO_4)$ **3** in acetonitrile. Inset: observed and calculated isotopic pattern for $[(BP)_2)CuCl]^+$ ($m/z = 670$).

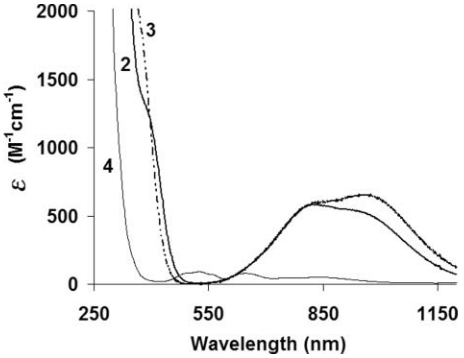

Fig. 6 Electronic absorption spectra of **2–4** (~1.2 mM) in CH_2Cl_2.

donor atoms in metal complexes is displaced by a strong coordinating external ligand or solvent. Such hemilabile ligands often possess varied strength of donor ability.[34] The hemilability of ligand BP with Cu(II), in solution, was revealed by electronic absorption spectroscopy. The molar intensity of complex **2** in non-coordinating solvent, CH_2Cl_2, is almost reduced to half in coordinating solvent, DMF (Fig. 7).

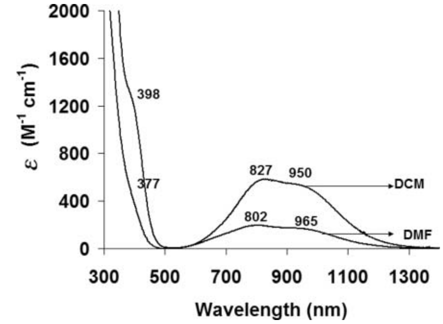

Fig. 7 The absorption spectrum of **2** (1.64 mM) in CH_2Cl_2 and DMF.

This is attributed to the relaxation of the constrained geometry about Cu(II) due to decoordination of the hindered tertiary amine-N of BP, with concomitant coordination of DMF (Scheme 1).

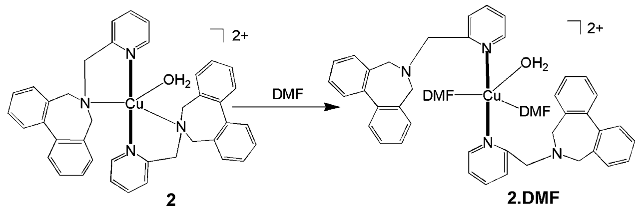

Scheme 1 Formation of DMF adduct, from complex **2**.

This change is possible as the tertiary amine-nitrogen possessing biphenyl crowd is weakly-coordinated to copper(II) ($Cu–N_{amine}$ = 2.16 Å) and gets replaced by DMF (Scheme 1). The change in solvent dielectricity from DCM to DMF could play a role in solution during this change. However, the overall band shape is unchanged retaining the same TBP geometry.

There are reports where the removal of the amine-nitrogen is aided by surrounding ligands.[35] Frequently, water exchange in five-coordinate copper(II) aqua complexes mainly occur at the more distant, labialized axial position and the steric effects decrease the water lability.[36] However, in complex **2** the coordinated water is strongly bonded to Cu(II) (2.09 Å) and water lability is not more facile. Furthermore, UV-vis spectral titration of **2** in CH_2Cl_2 with DMF (Fig. 8) and kinetics analysis suggest binding of two molecules of DMF (Fig. 8, inset) from which the binding constant (K_b) was determined. The binding affinity (K_b) of DMF is given by, $K_b = [(BP)_2Cu(OH_2)(DMF)_2]/[\{(BP)_2Cu(OH_2)\}^{2+}][DMF]^2$.

From the absorption spectra, it is known that $(A_0 - A)/(A - A_\infty) = 0.00164K_b[DMF]^2$, where, A_0 = absorbance (at 827 nm) of **2** in 100% DCM; A_∞ = absorbance (at 827 nm) of **2** in 100% DMF and $[\{(BP)_2Cu(OH_2)\}^{2+}$, **2**$] = 1.64 \times 10^{-3}$ M. The plot of $(A_0 - A)/(A - A_\infty)$ *vs.* $[DMF]^2$ gave a straight line passing through the origin (inset Fig. 8) with a slope of $1.64 \times 10^{-3} \times K_b$, from which $K_b = 92\ M^{-2}$ is calculated.

A similar observation with a bidentate with solvent effects leading to a change in spin-state with Ni(II) has been reported and the K_b values are much smaller (0.20 and 9.9 M^{-2}) compared to present values.[37]

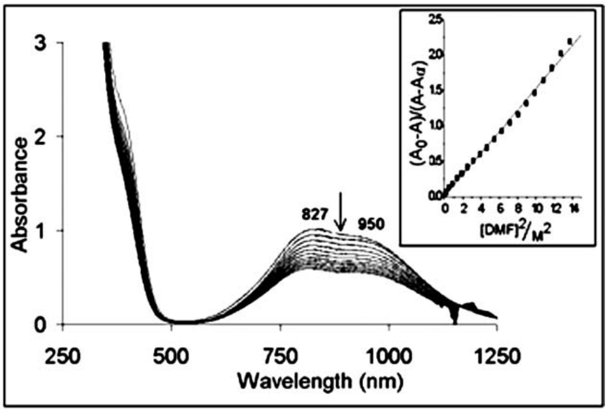

Fig. 8 Absorption spectral changes on controlled addition of DMF into CH_2Cl_2 solution of $[(BP)_2Cu(OH_2)](ClO_4)_2$ (1.64 mM) at 298 K. Change in volume $\Delta V < 5\%$. Inset: plot of $(Ao - A)/(A - A_\infty)$ *vs.* $[DMF]^2$.

(d) Monomer–dimer equilibrium: formation of dicopper dihydroxo complex. An attempted synthesis of the hydroxide analogue of **2**, *i.e.*, $[(BP)_2Cu(OH)]^+$ by the deprotonation of H_2O, using a base, triethylamine or tetramethylammonium hydroxide ($(CH_3)_4NOH$) gave instead the dimeric complex $[\{(BP)Cu\}_2(\mu\text{-}OH)_2]^{2+}$, **2a** (Scheme 2). Its formation was established by comparing the spectral features with that of an authentic sample of **2a** obtained from an independent synthesis.[38]

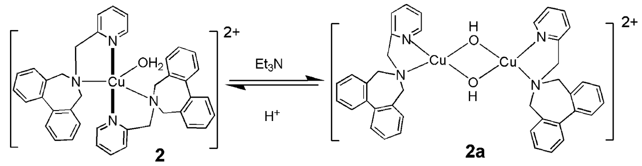

Scheme 2 The proposed monomer–dimer equilibrium between **2** and **2a**.

This conversion could be monitored by electronic absorption spectroscopy (Fig. 9). Controlled addition of a solution of NEt_3 in DMF to the aqua complex **2** in a 1 : 1 mixture of DMF : H_2O resulted in a gradual decrease in the absorbance of the initial spectrum, with associated growth of a new band at λ_{max} 622 nm, which corresponds to the dihydroxide-bridged dicopper(II) complex, **2a**. After complete addition of one equivalent of NEt_3 in DMF, no more apparent changes in the spectrum were observed.

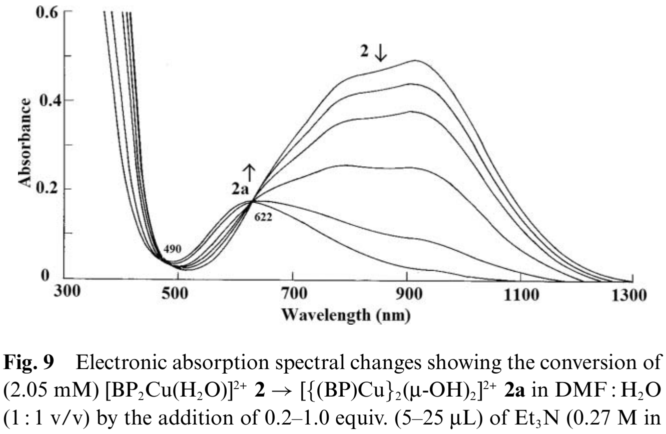

Fig. 9 Electronic absorption spectral changes showing the conversion of (2.05 mM) $[BP_2Cu(H_2O)]^{2+}$ **2** → $[\{(BP)Cu\}_2(\mu\text{-}OH)_2]^{2+}$ **2a** in DMF : H_2O (1 : 1 v/v) by the addition of 0.2–1.0 equiv. (5–25 μL) of Et_3N (0.27 M in DMF).

A clean conversion of **2** to **2a** is evident by the presence of two isosbestic points at 490 and 622 nm. In general, the simple deprotonation of a dimeric diaqua complex to a dimeric dihydroxo complex is quite common.[39] Also, the deprotonation of mononuclear copper(II)-aqua complexes to monomeric-hydroxo complexes in solution is known.[19,40] However, what we have observed in our study is interesting as it involves the formation of dimeric dihydroxo complex, **2a** (1 : 1 BP : Cu), from the mononuclear aqua complex (2 : 1 BP : Cu) with a base. This is rather uncommon as it requires elimination of a molecule of BP, followed by reorganization to the new complex. The presence of excess ligand was confirmed by thin layer chromatography (TLC).

A similar titration with the mononuclear chloro complex **3** with tetramethyl ammonium hydroxide, demonstrates the formation of a dinuclear dihydroxo complex **2a** (λ_{max} ~ 622 nm), which is in equilibrium with **3** (split band at 824 and 964 nm) (Fig. 10). To our knowledge, this is the first example of such a conversion observed.

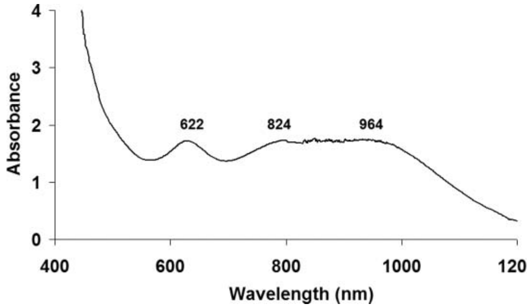

Fig. 10 Electronic absorption spectrum of the equilibrium mixture (~3 mM based on [**3**]) obtained from the reaction of $[BP_2Cu(Cl)]^+$, **3** with $(CH_3)_4NOH$ in EtOH.

(e) Dynamic NMR of 1. The Zn(II)-BP complex, $[(BP)_2Zn(OH_2)](ClO_4)_2$ **1**, in solution exhibits structural dynamics, which were studied by variable temperature ^1H NMR spectroscopy (Fig. 11). In general, the benzylic protons of the bridged biphenyl are chemically equivalent and appear as a singlet at room temperature. The non-equivalence of these protons displays an AB quartet at relatively lower temperatures. This is due to the restricted rotation about the atropisomeric C_{Ar}–C_{Ar} bond, resulting in two diastereomeric conformers.[41] However, the energy barrier is not sufficiently high enough to allow resolution of the enantiomeric conformations at room temperature, and these ligands are considered to be configurationally dynamic. In general, disubstituted biphenyls are resolvable only if two large *ortho* substituents are present or with certain bridges between the 2 and 2′ positions.[10] As seen, at room temperature (296 K), the ^1H NMR spectrum of free ligand BP, (bottom most spectrum in Fig. 11), shows two sharp singlets at 3.3 and 3.8 ppm in a 2 : 1 ratio for the methylene protons attached to the biphenyl and pyridyl rings. For the Zn(II) complex, the corresponding signals appear at 3.6 and 4.4 ppm respectively, at the same temperature; also the signals are relatively broad and down-field shifted compared to free BP. However, at 233 K, both the signals are separated into three AB quartets with six doublets at 3.7, 3.9, 4.2, 4.6 ppm with the broader one at ~3 ppm.

The relationship $\Delta G^{\#} = RT_c(22.96 + \ln(T_c/\sqrt{(\Delta\nu^2 + 6J^2)}))$ is used to determine the activation energy $\Delta G^{\#}$, from the coalescence

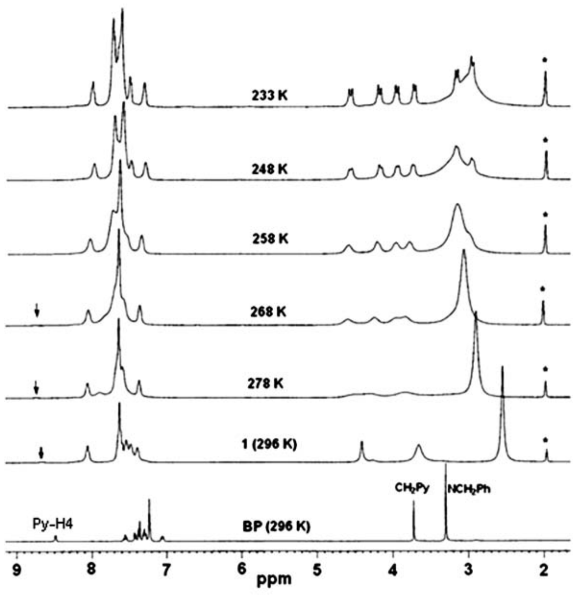

Fig. 11 ^{1}H NMR of the methylene region of $[(BP)_2Zn(OH_2)](ClO_4)_2$ **1** in CD_3CN, as a function of temperature.

temperature, T_c.[42] The calculated free energy for the inversion of bridged biphenyls is ~13.08 kcal mol^{-1} ($T_c = 273$ K, $\Delta\nu = 82.8$ Hz, $J = 8.7$ Hz) and for the pyridyl methylene (NCH_2PY) is ~12.37 kcal mol^{-1} ($T_c = 265$ K, $\Delta\nu = 152$ Hz, $J = 11.8$ Hz). It is proposed that the hindered rotation through C–C biaryl axis with the biphenyl seven-membered ring (Fig. 12(a)) results in two different conformations at low temperature. The coordination of Zn to nitrogen donors brings additional hindrance to biaryl ring (R) as shown by the five-membered ring flipping (Fig. 12(b)). Altogether, the combined effects reflect the higher activation barrier compared to free ligand BP with $\Delta G^{\#} = 10.3$ kcal mol^{-1}. The obtained values are comparable with reported biaryl systems with different substituents.[23,42,43]

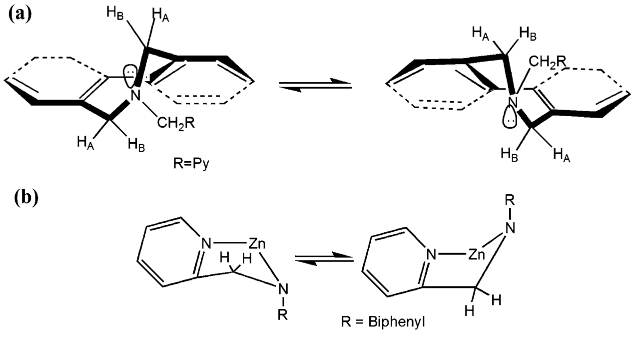

Fig. 12 The proposed dynamics for the (a) seven- and (b) five-membered ring flipping in **1**.

(f) ^{1}H NMR spectra of 2–4. The proton NMR spectra of complexes **2** and **3** in solution are broad and featureless, typical of mononuclear copper(II) centers due to their slow electronic relaxation (~10^{-8} s). On the other hand, the cobalt(II) complex **4**, shows relatively sharp signals, but are hyperfine shifted over a wide spectral window of −30 to 220 ppm (Fig. 13) due to the favorable electron relaxation of the high-spin Co(II) center. The ligand protons due to the pyridyl and methylene groups, which are closer to the Co(II) center, experience a more paramagnetic effect. The observed paramagnetic shifts are predominantly contact in origin as reflected in the observation that the majority of the signals are in one direction, all downfield shifted.

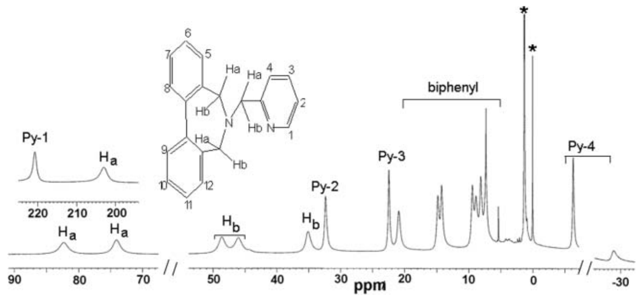

Fig. 13 ^{1}H NMR spectrum of **4** in $CDCl_3$ (* = TMS and solvent impurity).

A tentative assignment of signals was made based on one of our earlier reports.[44] The far downfield shifted signals are due to the pyridyl and methylenes which are close (Co–H ~3.0–3.8 Å) to the cobalt(II) center; the biphenyl protons which are far away (Co–H ~6.0–8.1 Å) appear in the region 5–15 ppm; the two up-field shifted signals are possibly due to the small spin-orbit coupling contribution. The spectral features are typical of a high-spin cobalt(II) complex. Complete assignment of the spectrum is beyond our current capabilities and is perhaps best left to a later study.

(g) Magnetism and EPR. The solution magnetic moment values of **2–4** were measured by Evans NMR method[12] and agree with the expected mononuclear structure. A value of 1.76 and 1.81 BM/Cu(II) noted for **2** and **3**, respectively, are close to a spin-only value, expected for Cu(II) ($S = 1/2$). Similarly, 4.47 BM/Co(II) of complex **4** is greater than the spin-only value for Co(II) ($S = 3/2$) and it is attributable to the spin-orbit coupling. The larger value is probably due to the biphenyl ligand which delocalizes electron density such that the separation of the electronic ground- and excited-states is decreased. This would give some orbital contribution to the magnetic moment, and would account for the greater than spin-only values.

The solution EPR spectra of **2** and **3** in CH_2Cl_2 : toluene (1 : 1, v/v) as a frozen glass at 77 K are shown in Fig. 14 (Table 4). Both of them show spectra typical of Cu(II) in TBP geometry with the unpaired electron residing in the d_{z^2} orbital.[40,45]

The spectral features of complex **3** are well-resolved, with $g_{\parallel} = 1.987$, $A_{\parallel} = 85$ G; $g_{\perp} = 2.200$, $A_{\perp} = 90$ G and in agreement with the geometry observed in the solid state; and also comparable with monomeric copper complexes with alkyl pyridyl ligands with TBP geometry in contrast to square pyramid geometry with similar ligands.[45b] Though a rhombic spectral pattern with $g_1 = 2.233$, $A_1 = 100$ G; $g_2 = 2.064$ G, $A_2 = 100$ G; $g_3 = 2.020$, $A_3 = 90$ was observed for **2**, they are broad and unresolved which may be due to vibronic coupling.[45a]

4. Redox properties

The redox properties of $[(BP)_2Cu(H_2O)]^{2+}$ **2** and $[(BP)_2Cu(Cl)]^{+}$ **3** in DMF were measured by cyclic voltammetry and the results are compared with the analogous complexes.[45c] As a representative example, the voltammogram of chloro-complex **3** is shown in

Table 4 Selected spectroscopic data for complexes **2–5**

	IR/cm^{-1}			EPR^b		
Complex	ν_{OH_2}	$\nu_{ClO_4^-}$	λ/nm (ε, M^{-1} cm^{-1})	g	A/G	μ/M(II) (BM)^a
2	3420	1094	398 (1250) 827 (586) 950 (530)	$g_1 = 2.233$ $g_2 = 2.064$ $g_3 = 2.020$	$A_1 = 100$ $A_2 = 100$ $A_3 = 90$	1.76
3	3487	1097	369 (1948) 824 (587) 964 (650)	$g_\parallel = 1.987$ $g_\perp = 2.200$	$A_\parallel = 85$ $A_\perp = 90$	1.81
4	—	1101	481 (74) 520 (90) 640 (79) 848 (51)	—	—	4.47
5	—	—	486 (46) 568 (93) 652 (144) 870 (24)	—	—	4.64

^{a} In CD_3CN (**2**); CD_3NO_2 (**3**); $CDCl_3$ (**4**); ^{b} CH_2Cl_2:toluene (1:1)

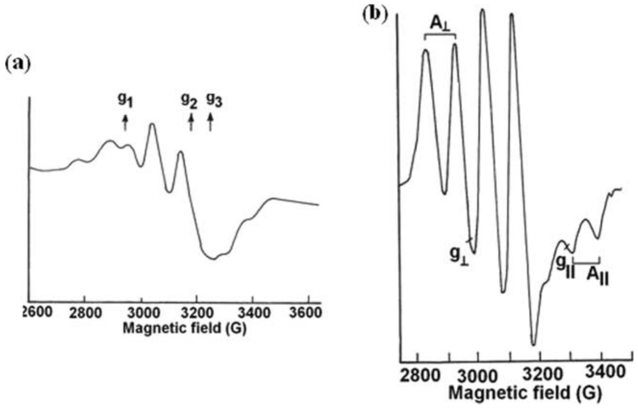

Fig. 14 EPR spectra of (a) $[(BP)_2Cu(H_2O)]^{2+}$ **2** and (b) $[(BP)_2Cu(Cl)]^+$ **3** in 1 : 1 CH_2Cl_2 : toluene at 77 K, scan range = 2200–4200 G, microwave frequency = 9.19 GHz, mod. amplitude 5 G, mod. frequency = 50 KHz (**2**) and 100 KHz (**3**), microwave power = 5 mW (**2**) and 10 mW (**3**).

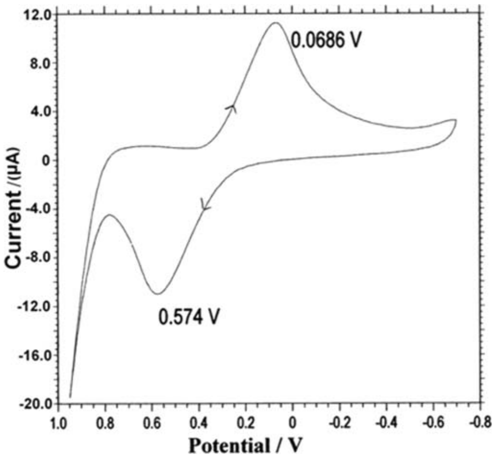

Fig. 15 Cyclic voltammogram of $[(BP)_2Cu(Cl)]^+$ **3** (~1 mM) in DMF. [Potentials are referenced *vs.* Ag/AgCl; scan rate: 50 mV s^{-1}; the ligand is redox inactive in the region, 0 to −1.5 V.]

Fig. 15. Complex **3** displays an irreversible redox wave with the E_c (cathodic potential) of 0.07 V and E_a (anodic potential) of 0.57 V *vs.* Ag/AgCl. A similar profile ($E_c = 0.12$ and $E_a = 0.55$ V) was also noted for **2**. The more positive value for the oxidation of Cu(I) to Cu(II) reflects the change in geometry from tetrahedral (Td) to TBP which is associated with reduced Cu(I) species.

Due to the hemilabile nature of BP in DMF, the initial copper(II) complex is in the form of a DMF adduct. When it undergoes reduction, expulsion of DMF leads to Cu(I) with a preferred Td geometry and reoxidation again involves solvent recoordination. This structural reorganization could be the reason for the large potential difference as observed in many mononuclear copper systems. The effect of solvent coordination in the redox behavior of mononuclear Cu(II) with tren ligand[32] and iminopyridyl ligand[46] is an additional support for the present study.

Conclusions

In summary, we have studied the five-coordinate Zn(II), Cu(II) and Co(II) complexes with unique trigonal bipyramidal geometry driven by a new biphenyl appended N-bidentate ligand. The crystal structures reveal the non-planar biphenyl twist compared to the almost planar bipyridyl twist in analogous mononuclear complexes. All complexes were studied by analytical and combined spectroscopic methods (UV-vis, IR, EPR, solution magnetic and ESI-MS). The spectral data were consistent with the TBP structure from X-ray analysis. The VT-^{1}H NMR study of the zinc-aqua complex, demonstrated the atropisomeric biphenyl dynamics in solution and the calculated free energy was in the low energy barrier as expected. Competitive binding studies in coordinating solvent like DMF proposes the replacement of two tertiary nitrogens from independent ligands, BP of complex **2**. Interestingly, a rare example of the conversion of Cu(II)-aqua complex $[(BP)_2Cu(OH_2)_2]^{2+}$ having ligand : Cu(II) in 2 : 1 ratio, to hydroxide-bridged dicopper(II) $[\{(BP)(Cu)\}_2(\mu\text{-}OH)_2]^{2+}$ containing ligand : Cu(II) in 1 : 1 ratio, was highlighted. Further studies involving the effect of coordinating solvents and isolation of solvent coordinated mononuclear complexes are underway in our laboratory.

Acknowledgements

The authors acknowledge Dr M. S. Moni, Sophisticated Analytical Instrumentation facility, Indian Institute of Technology, Madras, India for variable temperature NMR data. S. S. thanks the Council of Scientific and Industrial Research-University Grants Commission (CSIR-UGC), Government of India for financial assistance.

Notes and references

1 (*a*) R. H. Holm and E. I. Solomon, *Chem. Rev.*, 2004, **104**, 347–1200; (*b*) G. Parkin, *Chem. Rev.*, 2004, **104**, 699.
2 (*a*) J. P. Klinman, *J. Biol. Chem.*, 2006, **281**, 3013; (*b*) P. Chen and E. I. Solomon, *Proc. Natl. Acad. Sci. U. S. A.*, 2004, **101**, 13105; (*c*) S. T. Prigge, B. A. Eipper, R. E. Mains and L. M. Amzel, *Science*, 2004, **304**, 864; (*d*) J. P. Evans, A. Kyunghye and J. P. Klinman, *J. Biol. Chem.*, 2003, **278**, 49691.
3 N. Mitic, S. J. Smith, A. Neves, L. W. Guddat, L. R. Gahan and G. Schenk, *Chem. Rev.*, 2006, **106**, 3338.
4 (*a*) S. Tanase, I. A. Koval, B. Elisabeth, R. Gelder and J. Reedijk, *Inorg. Chem.*, 2005, **44**, 7860; (*b*) P. Comba and B. Bodo Martin, *Modeling of Macrocyclic Ligand Complexes; Macrocyclic Chemistry*, Springer, Netherlands, 2005, p. 303; (*c*) P. Comba and A. Lienke, *Inorg. Chem.*, 2001, **40**, 5206; (*d*) R. J. P. Williams, *Eur. J. Biochem.*, 1995, **234**, 363; (*e*) P. Comba, *Coord. Chem. Rev.*, 2000, **200–202**, 217; (*f*) P. Comba, *Coord. Chem. Rev.*, 1999, **185–186**, 81; (*g*) B. L. Vallee, J. F. Riordan, J. L. Bethune, T. L. Coombs, D. S. Auld and M. Sokolovsky, *Biochemistry*, 1968, **7**, 3547; (*h*) P. Comba, *Coord. Chem. Rev.*, 1999, **182**, 343; (*i*) H. B. Gray, B. G. Malmstrom and R. J. P. Williams, *JBIC, J. Biol. Inorg. Chem.*, 2000, **5**, 551; (*j*) S. Larsson, *JBIC, J. Biol. Inorg. Chem.*, 2000, **5**, 560; (*k*) U. Ryde, M. H. M. Olsson, B. O. Roos, J. O. A. De Kerpel and K. J. Pierloot, *JBIC, J. Biol. Inorg. Chem.*, 2000, **5**, 565; (*l*) U. Ryde, M. H. M. Olsson, K. Pierloot and B. O. Roos, *J. Mol. Biol.*, 1996, **261**, 586; (*m*) E. I. Solomon, M. D. Lowery, J. A. Guckert and L. B. LaCroix, in *Electron-Transfer Reactions-Inorganic, Organometallic and Biological Applications*, ed. S. S. Issied, American Chemical Society, Washington, DC, 1997, vol. 253, p. 317; (*n*) N. Shibata, T. Inoue, C. Nagano, N. Nishio, T. Kohzuma, K. Onodera, F. Yoshizaki, Y. Sugimura and Y. Kai, *J. Biol. Chem.*, 1999, **274**, 4225; (*o*) D. J. Berger and J. R. Telford, *Inorg. Chim. Acta*, 2002, **341**, 132.
5 (*a*) D. Maiti, H. C. Fry, J. S. Woertink, M. A. Vance, E. I. Solomon and K. D. Karlin, *J. Am. Chem. Soc.*, 2007, **129**, 264; (*b*) A. L. Gavrilova and B. Bosnich, *Chem. Rev.*, 2004, **104**, 349; (*c*) N. Kitajima and N. Morooka, *Chem. Rev.*, 1994, **94**, 737; (*d*) E. A. Lewis and W. B. Tolman, *Chem. Rev.*, 2004, **104**, 1047; (*e*) V. Mahadevan, Z. Hou, A. P. Cole, D. E. Root, T. K. Lal, E. I. Solomon and T. D. P. Stack, *J. Am. Chem. Soc.*, 1997, **119**, 11996.
6 (*a*) M. Colaneri and J. Peisach, *J. Am. Chem. Soc.*, 1992, **114**, 5335; (*b*) D. R. McMillin and H. R. Engeseth, in *Biological & Inorganic Copper Chemistry*, ed. K. D. Karlin and J. Zubieta, Adenine Press, New York, 1984, vol. 1, pp. 1–10; (*c*) B. R. M. Reinhammer, in *Copper Proteins and Copper Enzymes*, ed. R. Lontie, CRC Press, Boca Raton, FL, 1984, vol. 3, pp. 1–35; (*d*) W. B. Tolman and D. J. E. Spencer, *Curr. Opin. Chem. Biol.*, 2001, **5**, 188; (*e*) K. D. Karlin, D.-H. Lee, S Kaderli and A. D. Zuberbuhler, *Chem. Commun.*, 1997, 475.
7 (*a*) D. J. E. Spencer, N. W. Aboelella, A. M. Reynolds, P. L. Holland and W. B. Tolman, *J. Am. Chem. Soc.*, 2002, **124**, 2108; (*b*) N. W. Aboelella, E. A. Lewis, A. M. Reynolds, W. W. Brennessel, C. J. Cramer and W. B. Tolman, *J. Am. Chem. Soc.*, 2002, **124**, 10660; (*c*) A. F. A. Peacock, O. Iranzo and V. L. Pecoraro, *Dalton Trans.*, 2009, 2271.
8 S. Teramae, T. Osako, S. Nagatomo, T. Kitagawa, S. Fukuzumi and S. Itoh, *J. Inorg. Biochem.*, 2004, **98**, 746.
9 (*a*) S. G. Telfer, T. Sato, T. Harada, R. Kuroda, J. Lefebvre and D. B. Leznoff, *Inorg. Chem.*, 2004, **43**, 6168; (*b*) E. H. Alilou, A. El Hallaoui, E. H. El Ghadraoui and M. Pierrot, *Z. Kristallogr. New Cryst. Struct.*, 1999, **214**, 213; (*c*) M. Saporita, G. Bottari, G. Brancatelli, D. Drommi, G. Bruno and F. Faraone, *Eur. J. Inorg. Chem.*, 2008, 59; (*d*) C. Vedder, F. Schaper, H. Brintzinger, M. Kettunen, S. Babik and G. Fink, *Eur. J. Inorg. Chem.*, 2005, 1071; (*e*) P. T. Kaye, T. Nyokong, G. M. Watkins and K. W. Wellington, *ARKIVOC*, 2002, **IX**, 9; G. J. P. Britovsek, J. England and A. J. P. White, *Dalton Trans.*, 2006, 1399.
10 (*a*) P. J. Walsh, A. E. Lurain and J. Balsells, *Chem. Rev.*, 2003, **103**, 3297; (*b*) A. M. Costa, C. Jimeno, J. Gavenonis, P. J. Carroll and P. J. Walsh, *J. Am. Chem. Soc.*, 2002, **124**, 6929; (*c*) E. L. Eliel and S. H. Wilen, *Stereochemistry of Organic Compounds*, Wiley & Sons, New York, 1994.
11 D. D. Perrin, W. L. Armarego and D. R. Perrin, *Purification of Laboratory Chemicals*, Pergamon, New York, 2nd edn, 1980.
12 D. F. Evans, *J. Chem. Soc.*, 1959, 2003.
13 S. Sabiah, *Ph.D. Thesis*, Indian Institute of Technology Madras, India, October, 2007.
14 *Enraf-Nonius CAD-4 Software*. Version 5.0. Enraf-Nonius, Delft, Netherlands, 1989.
15 A Altomare, G. Cascarano, C. Giacovazzo and A. Guagliardi, *J. Appl. Crystallogr.*, 1993, **26**, 343.
16 G. M. Sheldrick, *SHELX93, Program for Crystal Structure Refinement*, University of Göttingen, Germany, 1997.
17 L. J. Farrugia, *J. Appl. Crystallogr.*, 1997, **30**, 565.
18 S. Sabiah, B. Varghese and N. N. Murthy, *J. Chem. Crystallogr.*, 2006, **36**, 147.
19 (*a*) S. C. Lee and R. H. Holm, *J. Am. Chem. Soc.*, 1993, **115**, 11789; (*b*) Y. Yamada, H. Sakurai, Y. Miyashita, K. Fujisawa and K. Okamoto, *Polyhedron*, 2002, **21**, 2143.
20 (*a*) C. Kaes, A. Katz and M. W. Hosseini, *Chem. Rev.*, 2000, **100**, 3553; (*b*) P. M. F. J. Costa, M. Mora, M. J. Calhorda, V. Felix, P. Ferreira, M. G. B. Drew and H. Wadepohl, *J. Organomet. Chem.*, 2003, **687**, 57.
21 (*a*) D. C. Iffland and H. Siegel, *J. Am. Chem. Soc.*, 1958, **80**, 1947; (*b*) J. Edwards, G. Robin and T. W. Wallace, *Acta Crystallogr., Sect. B: Struct. Sci.*, 2005, **61**, 335; (*c*) A. C. Benniston, A. Harriman, P. V. Patel and C. A. Sams, *Eur. J. Org. Chem.*, 2005, 4680; (*d*) Andrea Mazzanti, Lodovico Lunazzi, Mirko Minzoni and J. Edgar Anderson, *J. Org. Chem.*, 2006, **71**, 5474.
22 (*a*) F. Leroux, M. Maurin, N. Nicod and R. Scopelliti, *Tetrahedron Lett.*, 2004, **45**, 1899; (*b*) L. Eshdat, E. Shabtai, S. A. Saleh, T. Sternfeld, M. Saito, Y. Okamoto and M. Rabinovitz, *J. Org. Chem.*, 1999, **64**, 3532; (*c*) D. Casarini, L. Lunazzi, M. Mancinelli, A. Mazzanti and C. Rosini, *J. Org. Chem.*, 2007, **72**, 7667.
23 S. Superchi, D. Casarini, A. Laurita, A. Bavoso and C. Rosini, *Angew. Chem., Int. Ed.*, 2001, **40**, 451.
24 F. X. Gomis-Ruth, W. Stocker, R. Huber, R. Zwilling and W. Bode, *J. Mol. Biol.*, 1993, **229**, 945.
25 (*a*) G. Murphy, C. Murphy and B. Hathaway, *J. Chem. Soc., Dalton Trans.*, 1997, 2653; (*b*) H. Nagao, N. Komeda, M. Mukaida, M. Suzuki and K. Tanaka, *Inorg. Chem.*, 1996, **35**, 6809.
26 Y. B. Wei and P. Yang, *Acta Crystallogr., Sect. E: Struct. Rep. Online*, 2004, **60**, m429.
27 P. Nagle, E. Sullivan, B. J. Hathaway and E. Muller, *J. Chem. Soc., Dalton Trans.*, 1990, 3399.
28 K. D. Karlin, J. C. Hayes, S. Juen, P. J. Hutchinson and J. Zubieta, *Inorg. Chem.*, 1982, **21**, 4106.
29 (*a*) R. R. Holmes, *Acc. Chem. Res.*, 1979, **12**, 257; (*b*) R. R. Holmes and J. A. Deiters, *J. Am. Chem. Soc.*, 1977, **99**, 3318.
30 W. M. Davis, S. J. Dzugan, M. W. Glogowski, R. Delgado and D. H. Busch, *Inorg. Chem.*, 1991, **30**, 2724.
31 A. W. Addison, T. N. Rao, J. Reedijk, J. Rijn and G. C. Verschoor, *J. Chem. Soc., Dalton Trans.*, 1984, 1349.
32 (*a*) G. Izzet, B. Douziech, T. Prange, A. Tomas, I. Jabin, Y. L. Mest and O. Reinaud, *Proc. Natl. Acad. Sci. U. S. A.*, 2005, **102**, 6831; (*b*) K. J. Tubbs, A. L. Fuller, B. Bennett, A. M. Arif and L. M. Berreau, *Inorg. Chem.*, 2003, **42**, 4790; (*c*) T. Suresh and B. J. Hathaway, *J. Chem. Soc., Dalton Trans.*, 1981, 2029.
33 (*a*) G. Achilleas, K. Spyridoula and P. R. Catherine, *Inorg. Chem. Commun.*, 2000, **3**, 251; (*b*) J.-W. Lim, M. Mikuriya and H. Sakiyama, *Bull. Chem. Soc. Jpn.*, 2001, **74**, 2131; (*c*) I. Bertini, D. Gatteschi and A. Scozzafava, *Inorg. Chem.*, 1975, **14**, 812.
34 C. S. Slone, D. A. Weinberger and C. A. Mirkin, in Transition metal coordination chemistry of hemilabile ligands, *Progress in Inorganic Chemistry*, ed. K. D. Karlin, John Wiley & Sons Inc., 1999, vol. 48, pp. 233–350.
35 (*a*) F. Thaler, C. D. Hubbard, F. W. Heinemann, R. V. Eldik, S. Schindler, I. Fabian, A. M. Dittler-Klingemann and F. E. Hahn, *Inorg. Chem.*, 1998, **37**, 4022; (*b*) L. Li, A. A. N. Sarjeant and K. D. Karlin, *Inorg. Chem.*, 2006, **45**, 7160.
36 A. Neubrand, F. Thaler, M. Korner, A. Zahl, C. D. Hubbard and R. V. Eldik, *J. Chem. Soc., Dalton Trans.*, 2002, 957.
37 H. Ohtsu and K. Tanak, *Inorg. Chem.*, 2004, **43**, 3024.

38 S. Sabiah, B. Varghese and N. N. Murthy, *Chem. Commun.*, 2009, 5636.
39 G. Battaini, L. Casella, M. Gullotti, E. Monzani, G. Nardin, A. Perotti, L. Randaccio, L. Santagostini, F. W. Heinemann and S. Schindler, *Eur. J. Inorg. Chem.*, 2003, 1197.
40 L. M. Berreau, S. Mahapatra, J. A. Halfen, V. G. Young and W. B. Tolman, *Inorg. Chem.*, 1996, **35**, 6339.
41 I. O. Sutherland and M. V. Ramsay, *Tetrahedron*, 1965, **21**, 3401.
42 L. Vial and J. Lacour, *Org. Lett.*, 2002, **4**, 3939.
43 S. Superchi, R. Bisaccia, D. Casarini, A. Laurita and C. Rosini, *J. Am. Chem. Soc.*, 2006, **128**, 6893.
44 N. N. Murthy, K. D. Karlin, I. Bertini and C. Luchinat, *J. Am. Chem. Soc.*, 1997, **119**, 2156.
45 (*a*) K. Fujisawa, T. Kobayashi, K. Fujita, N. Kitajima, Y. Moro-oka, Y. Miyashita, Y. Yamada and K. I. Okamoto, *Bull. Chem. Soc. Jpn.*, 2000, **73**, 1797; (*b*) A. Wada, M. Harata, K. Hasegawa, K. Jitsukawa, H. Masuda, M. Mukai, T. Kitagawa and H. Einaga, *Angew. Chem., Int. Ed.*, 1998, **37**, 798; (*c*) B. Lucchese, K. J. Humphreys, D.-H. Lee, C. D. Incarvito, R. D. Sommer, A. L. Rheingold and K. D. Karlin, *Inorg. Chem.*, 2004, **43**, 5987 and references there in; (*d*) G. Kokoszka, K. D. Karlin, F. Padula, J. Baranowski and C. Goldstein, *Inorg. Chem.*, 1984, **23**, 4378; (*e*) R. Barbucci, A. Bencini and D. Gatteschi, *Inorg. Chem.*, 1977, **16**, 2117.
46 S. Dehghanpour, N. Bouslimani, R. Welter and F. Mojahed, *Polyhedron*, 2007, **26**, 154.